

# Atmospheric Processing Outside Clouds Increases Soluble Iron in Mineral Dust

Zongbo Shi,<sup>\*,†</sup> Michael D. Krom,<sup>‡,§</sup> Steeve Bonneville,<sup>‡,⊥</sup> and Liane G. Benning<sup>‡,||</sup>

<sup>†</sup>School of Geography, Earth and Environmental Sciences, University of Birmingham, Birmingham, U.K.

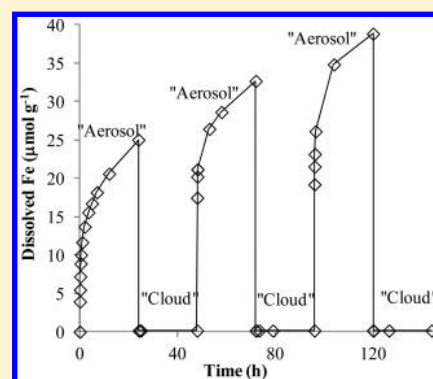
<sup>‡</sup>Cohen Geochemistry Laboratory, School of Earth and Environment, University of Leeds, Leeds, U.K.

<sup>§</sup>Charney School for Marine Science, Haifa University, Haifa, Israel

<sup>⊥</sup>Biogéochimie et Modélisation du système Terre, Département des Sciences de la Terre et de l'Environnement, Université Libre de Bruxelles, Brussels, Belgium

<sup>||</sup>GFZ German Research Centre for Geosciences, Telegrafenberg, D-14473 Potsdam, Germany

**ABSTRACT:** Iron (Fe) is a key micronutrient regulating primary productivity in many parts of the global ocean. Dust deposition is an important source of Fe to the surface ocean, but most of this Fe is biologically unavailable. Atmospheric processing and reworking of Fe in dust aerosol can increase the bioavailable Fe inputs to the ocean, yet the processes are not well understood. Here, we experimentally simulate and model the cycling of Fe-bearing dust between wet aerosol and cloud droplets. Our results show that insoluble Fe in dust particles readily dissolves under acidic conditions relevant to wet aerosols. By contrast, under the higher pH conditions generally relevant to clouds, Fe dissolution tends to stop, and dissolved Fe precipitates as poorly crystalline nanoparticles. If the dust-bearing cloud droplets evaporated again (returning to the wet aerosol stage with low pH), those neo-formed Fe nanoparticles quickly redissolve, while the refractory Fe-bearing phases continue to dissolve gradually. Overall, the duration of the acidic, wet aerosol stage ultimately increases the amount of potentially bioavailable Fe delivered to oceans, while conditions in clouds favor the formation of Fe-rich nanoparticles in the atmosphere.



## INTRODUCTION

Iron (Fe) is a limiting micronutrient for phytoplankton growth in large parts of the global ocean.<sup>1,2</sup> A major external source of Fe to the open ocean is atmospheric aerosols, particularly Fe from dust.<sup>3</sup> Understanding the processes that control the dissolution of Fe in dust in the atmosphere has important implications for the global carbon cycle and for predicting climate.<sup>1,3,4</sup> Most of the Fe present in dust is as crystalline Fe oxides and within aluminosilicates including clays.<sup>5</sup> These minerals are poorly soluble in seawater, and thus, Fe in them is hardly bioavailable. The fraction generally considered bioavailable is the soluble Fe and poorly ordered Fe oxyhydroxide nanoparticles (Fe-NPs; ferrihydrite), the latter of which are used and are metabolically important for at least some phytoplankton species.<sup>6–9</sup>

The fractional Fe solubility in atmospheric aerosols (the fraction of dissolved to total Fe) ranges between <0.1% and 80%, but that of fresh dust is generally less than 0.5%.<sup>4</sup> There is strong evidence that atmospheric processing can at least partly explain the enhanced fractional Fe solubility in aerosols compared to fresh dust.<sup>4,5</sup> One of the important atmospheric reactions controlling these processes involves the changing chemical conditions in the water around mineral dust. Fresh dust particles emitted to the atmosphere can be chemically altered (aged) by acid processes involving sulfate and nitrate

uptake.<sup>10,11</sup> Under suitable conditions, both fresh and aged dust particles can be activated into clouds.<sup>12,13</sup> Acids such as sulfuric and nitric acid can be also formed in the cloud droplets, but this uptake only minimally changes the cloud pH because of the relatively high volume of water present. However, most clouds do not precipitate as rain but rather evaporate. During this evaporation, a thin film of water remains around dust particles. These particles are often called wet aerosol,<sup>14,15</sup> since they contain a small amount of water. A wet aerosol is defined as an aerosol that contains a thin film of water because of water uptake by hygroscopic materials at elevated relative humidity. The amount of water around such wet aerosol can increase with increasing relative humidity.<sup>16</sup> Once the relative humidity is increased over the supersaturation point, the wet aerosol particle will be activated and will become a cloud droplet. Only when the relative humidity is extremely low, that is, below the efflorescence relative humidity, will a wet aerosol particle become a dry particle. During its lifetime, a typical aerosol particle may experience several condensation/evaporation

Received: September 20, 2014

Revised: January 8, 2015

Accepted: January 9, 2015

Published: January 9, 2015

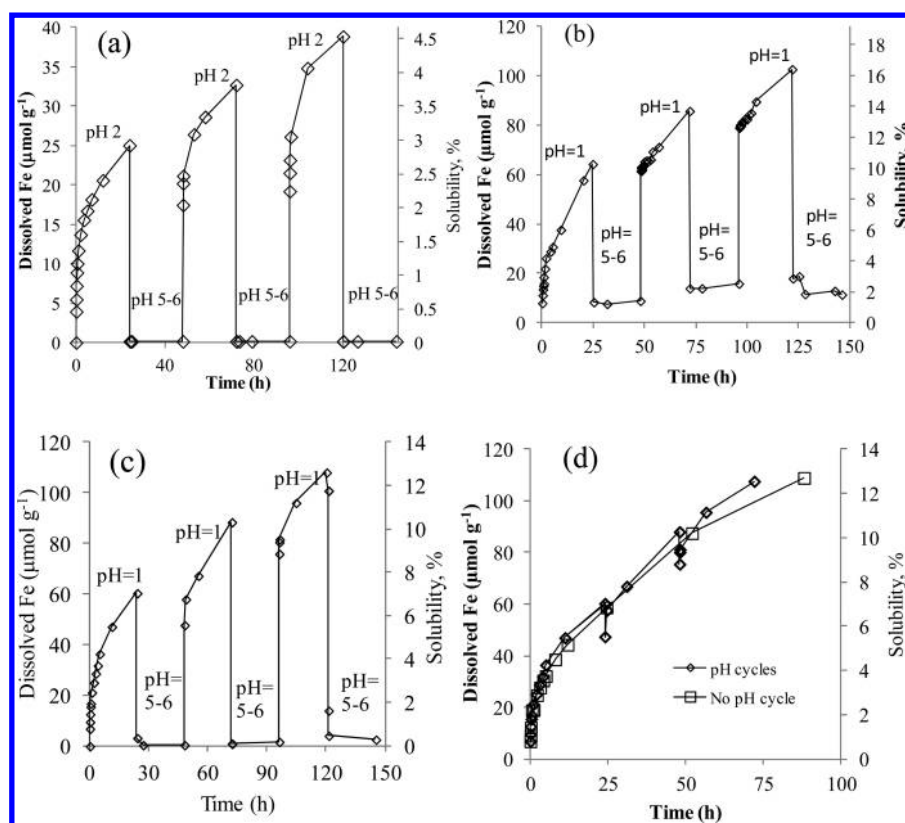


**Figure 1.** Change in dissolved Fe per gram of dust during simulated wet aerosol and cloud droplet processing for (a) Tibesti (pH 2 and pH 5–6; 333 mg dust per L), (b) Beijing (pH 1 and pH 5–6; 60 mg dust per L), and (c) Tibesti (pH 1 and pH 5–6; 60 mg dust per L) dusts and (d) comparison between the Fe dissolution curve of a Tibesti dust sample at pH 1 measured continuously (no pH cycling)<sup>30</sup> at 60 mg L<sup>-1</sup> with a cumulative curve from the experiment also at pH 1 shown in Figure 1c but with the high pH periods of the simulated cloud processing removed from the data.

cycles before being removed from the atmosphere as rain or through dry deposition.<sup>17</sup>

Besides the changes in water content, these condensation/evaporation cycles induce large variations in the chemistry of the water around the aerosol particles. While there are some exceptions (such as highly polluted areas) where cloud waters are highly acidic (e.g., pH 2.2),<sup>18</sup> generally, the pH of cloud waters is close to near-neutral, for example, above 4–5.<sup>19</sup> However, as cloud droplets evaporate, the pH in the forming wet aerosol decreases and the ionic strength increases. The pH in the water film around wet aerosol can be lower than 2.<sup>20–22</sup> Such pH variations between cloud droplets and wet aerosol are crucial because the solubility of Fe in mineral dust is strongly pH dependent.<sup>23–28</sup>

In this study, we report the results of a series of experiments that simulated the pH controlled processing of mineral dust as wet aerosols and as cloud droplets. We monitored the change in fractional Fe solubility in dust samples during cycling from low, wet aerosol pH to near-neutral, cloud droplet pH. On the basis of this and previous data, we developed a model to predict the changes in fractional Fe solubility as a function of water content surrounding dust particles, hence replicating *in silico* the transition from wet aerosols to cloud droplets.

## MATERIALS AND METHODS

Two samples were used in the experiments. The first sample was collected from a dry riverbed draining the Tibesti Mountains (South Libya; N25°35' E16°31'; hereafter called Tibesti). This is known to be a major source of the lithogenic

particles to the Bodele depression, which is presently the single largest Saharan dust source.<sup>29</sup> This sample was first dry-sieved to <63 μm and then was wet-sieved to <20 μm with ~50 mL of Milli-Q water (18.2 MΩ). The sample suspensions were freeze-dried and later were gently disaggregated before further experimentation. This procedure has been shown to have little impact on the Fe speciation and dissolution behavior at acidic pH.<sup>25</sup> The second sample was an Asian dry-deposited dust sample (hereafter termed Beijing dust), which was collected from a pre-cleaned surface on the campus of China University of Mining and Technology (Beijing, China (N 39°60', E 116°21')) after a superdust storm episode on April 17, 2006. For simplicity, both samples are described in the text as dust. All experiments were performed at room temperature (~298 K) under constant stirring (~50 rpm) and in dark conditions (wrapped in aluminum foil). In the Tibesti and Beijing dust, of the total Fe, Fe oxides represent 37.7% and 22.3%, respectively, with the remaining Fe being associated with primarily aluminosilicates.<sup>25</sup> Furthermore, the percentage of dissolved Fe released during ascorbate extraction, which solubilizes highly reactive Fe phase, especially ferrihydrite, was 0.63% and 1.71% of the total Fe content in the Tibesti and Beijing dust, respectively.<sup>25</sup>

Either 60 or 333 mg of dust was added to 1 L Milli-Q water that was preacidified to pH 2 or 1 with H<sub>2</sub>SO<sub>4</sub>. To simulate cycling between wet aerosol and cloud droplets, the dust suspensions were cycled three times between acidic (pH 2 or 1, 24 h) and near-neutral pH (pH 5–6, 24 h; pH raised by adding ammonium hydroxide) following the procedure of Shi et al.<sup>30</sup> H<sub>2</sub>SO<sub>4</sub> was used instead of HNO<sub>3</sub> to avoid the potential

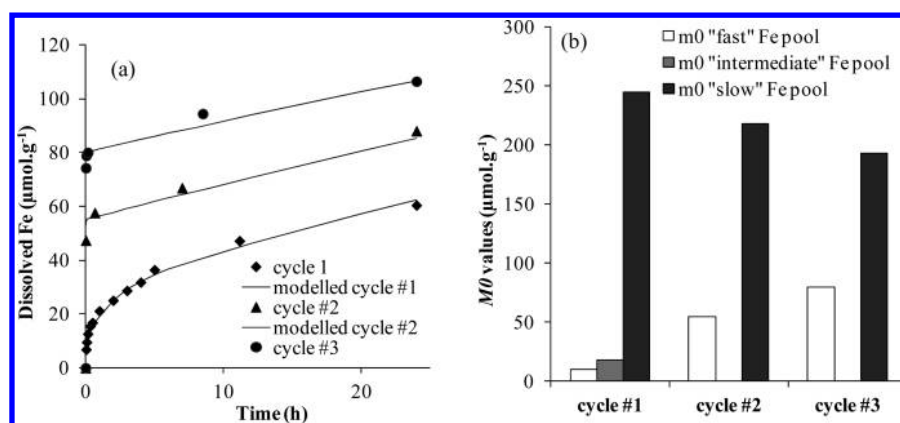


**Figure 2.** (a) Measured (symbols) and modeled (lines) dissolved Fe concentrations during the successive acidic stages of the three cycling experiments for Tibesti dust (Figure 1c). (b) Fitted  $M_0$  values for the three Fe pools (fast, intermediate, and slow) for each of the three successive acidic stages of the cycling experiments with Tibesti dust from pH 2 and 5–6. Note the fitting assumes that the sum of the three Fe pools is constant.

oxidation of dissolved Fe(II) by  $\text{NO}_3^-$ .<sup>27</sup> The amount of acid or base added to achieve these pH cycles was less than 1% of the total volume of the suspensions, and thus, they had negligible effect on the Fe concentration calculations. The ionic strength for the pH 1/2 and 5–6 increased from 0.15/0.015 mol  $\text{L}^{-1}$  in the first low pH cycle to a maximum of 0.5 mol  $\text{L}^{-1}$  in the third cycle. pH was measured with an accuracy of  $\pm 0.1$  pH unit. Dissolved Fe concentrations were measured regularly to follow the dissolution or reprecipitation of Fe phases. Aliquots of the dust suspensions and reacting solutions were separated by filtration through 0.2  $\mu\text{m}$  filters directly into HCl (final concentration 0.2 N HCl), and the aliquots were stored for a maximum of one month at 4  $^\circ\text{C}$  until Fe analysis (see below). Filtration through 0.2  $\mu\text{m}$  pore sized filters is commonly used for measurements of dissolved species from dust suspension, specially at near-neutral pH. Fe colloids tend to aggregate or adhere to mineral surface,<sup>31</sup> which are efficiently retained by a 0.2  $\mu\text{m}$  filter.

During cloud formation, the pH change around a dust particle is due to water uptake after the particle activation into a cloud droplet, which is an almost instantaneous process. To simulate this process in the laboratory, we prepared dust suspensions with 10 g dust per liter of water which were continuously stirred for 800 h in the dark as described above. Experiments were run in either (1) 1 L of a 0.005 mol  $\text{L}^{-1}$   $\text{H}_2\text{SO}_4$  (low ionic strength,  $I = 0.015$  mol  $\text{L}^{-1}$ ) solution or (2) 1 L of a 1 mol  $\text{L}^{-1}$   $(\text{NH}_4)_2\text{SO}_4$  and 0.05 mol  $\text{L}^{-1}$   $\text{H}_2\text{SO}_4$  (high  $I = 3.15$  mol  $\text{L}^{-1}$ ) solutions. Experiment 1 aimed at mimicking acidic pH dust dissolution at low  $I$  to compare with literature,<sup>23–25</sup> while experiment 2 is more representative of the atmospheric aerosol waters, that is, acidic pH and high  $I$ .<sup>20</sup> At the end of each experiment, 100  $\mu\text{L}$  of each dust suspension was diluted to 100 and 500 mL, respectively (1000 and 5000 times dilutions), with high-purity Milli-Q water. The final pH of the diluted solutions was 4.8 and 5.0, respectively. Six aliquots of each diluted dust suspension were sampled after 10 min, and after filtration (0.2  $\mu\text{m}$ ), the dissolved Fe concentrations were measured within 30 min.

Dissolved Fe concentration was measured in all cases using the spectrophotometric ferrozine method.<sup>32</sup> The solutions from the high  $I$  experiment were diluted 100 times with acidified Milli-Q water (0.1 mol  $\text{L}^{-1}$  HCl) before measurement to avoid interferences. Dissolved Fe measurements of six replicate filtrates from the Tibesti dust suspension experiments at pH

2 gave a precision of  $\pm 1.2\%$  (1 s,  $n = 6$ ). The detection limit for dissolved Fe is 0.05  $\mu\text{M}$ .

## RESULTS AND DISCUSSION

Figure 1a–c shows the fractional Fe solubility during experiments, which simulated the pH cycling of wet aerosol (acidic) and cloud processing (near-neutral) of Tibesti and Beijing dusts. During the first acidic pH cycle (at pH 2), dissolved Fe concentration for Tibesti dust (Figure 1a) increased to 25  $\mu\text{mol}\cdot\text{g}^{-1}$ . After the pH was raised to 5–6, the dissolved Fe concentration dropped in less than 1 min to below  $<0.15$   $\mu\text{mol}\cdot\text{g}^{-1}$  and remained constant until the pH was decreased again. During the second acidic cycle (pH 2), the dissolved Fe concentration increased to 17.5  $\mu\text{mol}\cdot\text{g}^{-1}$  (within 2.5 min), and in the subsequent 24 h, the dissolved Fe concentration reached 32.7  $\mu\text{mol}\cdot\text{g}^{-1}$ . When the pH was again increased to 5–6, the dissolved Fe concentration again rapidly dropped to  $<0.15$   $\mu\text{mol}\cdot\text{g}^{-1}$  and remained stable for 24 h. Finally, during the third acidic cycle, the dissolved Fe concentration increased to 38.8  $\mu\text{mol}\cdot\text{g}^{-1}$  after 24 h and decreased to  $<0.15$   $\mu\text{mol}\cdot\text{g}^{-1}$  after the pH was again increased. pH cycling experiments using either the Beijing dust (Figure 1b, between pH 1 and 5–6) or the Tibesti dust (Figure 1c, between pH 1 and 5–6) showed similar Fe dissolution and cycling behaviors despite the somewhat different Fe mineralogy and composition between these two samples.<sup>25</sup> Our experiments produced changes in dissolved Fe concentration similar to those of Spokes et al.<sup>23</sup> and Mackie et al.<sup>24</sup> However, our interpretation of the data is different. They considered that the Fe dissolution occurred mainly in clouds, while our data suggest that the dissolution occurs mainly in the wet aerosol stage.

When the pH was raised to 5–6, simulating the transition from wet aerosols into cloud droplets, the dissolved Fe precipitated as Fe nanoparticles (Fe-NPs).<sup>30</sup> Such Fe-NPs are highly reactive and similar in composition to ferrihydrite.<sup>30</sup> Indeed, at pH 5–6, the measured dissolved Fe concentration was  $<0.1$   $\mu\text{mol}\cdot\text{L}^{-1}$ , which is orders of magnitude lower than that at lower pH. For a 60 mg Tibesti dust per liter of solution, this Fe concentration is equivalent to a fractional Fe solubility of 0.2%. This low value is similar to previous laboratory studies showing that at pH  $> 4$ –5, only a small proportion of Fe in dusts, for example,  $<0.5\%$ , can be dissolved.<sup>24,26</sup>

We tested this behavior over three cycles each (Figure 1a–c) and observed a gradual increase in the maximum dissolved Fe

concentrations reached at the end of each acidic pH cycle. This shows that the neoformed Fe-NPs were quickly redissolved (within the first few minutes of the second and third acidic cycles). Furthermore, this behavior suggests that the less labile Fe-bearing minerals in dust, mostly crystalline Fe oxides, aluminosilicates, and clay minerals,<sup>25</sup> dissolve slowly yet continuously at acidic pH until the pH is raised again to pH 5–6 (Figure 1a–c). This dissolution/precipitation behavior was independent of dust source as similar overall patterns were observed with both the Beijing and Tibesti dusts. This behavior is also independent of the low pH (either 2 or 1) at which the experiments were carried out. We predict a similar trend if the dust was cycled between pH 3 and 5–6 as the acid solubility of Fe at pH 3 is orders of magnitude higher than that at pH 5–6 as shown in the pH-dependent dissolution experiments of Fe in dusts by Shi et al.,<sup>25</sup> Cwiertny et al.,<sup>27</sup> and Fu et al.<sup>28</sup>

Using a first-order kinetic model,<sup>25</sup> we fitted the changes in dissolved Fe concentrations at acidic pHs as a simultaneous dissolution of three Fe mineral pools (fast, intermediate, and slow). The values for  $M_0$  (initial Fe amount in any given pool) and  $k$  (rate constant) that we had previously determined for Tibesti dust<sup>25</sup> enabled us to fit reasonably well the time-evolution of the dissolved Fe concentrations during the first acidic wet aerosol stage (e.g., Figure 2a). However, during the second and third low pH cycles, the best fits were obtained by adjusting the values of  $M_0$  and  $k$  of the fast Fe pool (e.g., Figure 2). The  $k$  value was changed to the one determined previously<sup>25</sup> for fresh ferrihydrite. In our previous study, we showed through transmission electron microscopy (TEM) micrographs that in suspensions of dust and Fe oxide standard materials increasing the pH from 1 or 2 to pH 5–6 induce the formation of Fe-NPs (Figure 3 in ref 30). Thus, this explains in

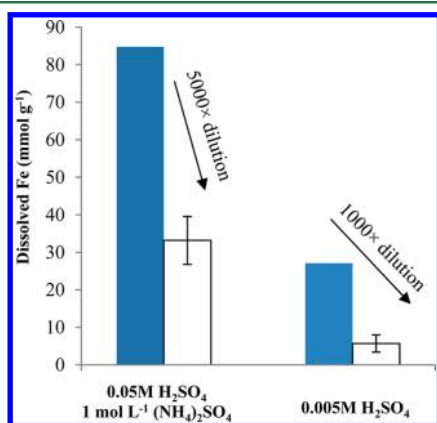


**Figure 3.** Decrease in dissolved Fe concentrations after 5000 and 1000 times dilution of an acidic dust suspension representing the transition from wet aerosol to cloud droplet conditions; error bars represent standard deviation of six replicates.

the second and third cycles of the current experiments why the amount of Fe in the fast pool ( $M_0$ ) increased by 3, 8, and 11 times for Tibesti (pH 2, Figure 1a), Tibesti (pH 1, Figure 1c), and Beijing (pH 1, Figure 1b) dust samples, respectively. Overall, our kinetic model indicates that there was a transfer of Fe from the low reactivity Fe pools (intermediate and slow Fe pools) into the highly reactive Fe-NPs (fast Fe pool) in the second and third cycles. This is consistent with the increase in Fe-NPs formed during the atmospheric processing of dust in each cycle and also fits with the previously observed Fe-NPs in natural dust-laden rainwater.<sup>30</sup>

The pH increase during the cloud droplet formation stage is not the result of the addition of an alkali but is rather due to the several orders of magnitude dilution by water. This dilution also results in an increased water/dust ratio and decreased ionic strength. The increasing water volume around wet aerosol has, however, antagonistic effects for Fe-NP formation; it lowers the dissolved Fe<sup>3+</sup> concentrations, hence preventing supersaturation to be reached, while at the same time shifts the pH toward near-neutral values where Fe has its minimum solubility. These effects on the fractional Fe solubility were tested experimentally by diluting acidic dust aerosol suspensions 1000 and 5000 times. Data in Figure 3 confirm the results of the Fe cycling experiments (Figure 1a–c) and further show that about 80% and 60% of the initial dissolved Fe in the high and low ionic strength dust suspensions were precipitated as Fe-NPs from the solution phase.

We also modeled the solubility of Fe oxides upon dilution (i.e., cloud droplet formation stage) using Visual MINTEQ (<http://www2.lwr.kth.se/English/Oursoftware/vminteq/>). Our initial conditions were the high ionic strength wet aerosol solution chemistry of Tibesti dust after 24 h at pH 1 (i.e., 236  $\mu\text{mol L}^{-1}$  dissolved Fe in 1 M (NH<sub>4</sub>)<sub>2</sub>SO<sub>4</sub>). The pH, ionic strength, and dissolved Fe<sup>3+</sup> concentrations in the diluted wet aerosol waters were calculated in order to derive the saturation index with respect to fresh ferrihydrite (solubility constant  $K_{sp} = 10^{1.9}$ )<sup>33</sup> for a 5–50 000 times dilution factor (Figure 4).

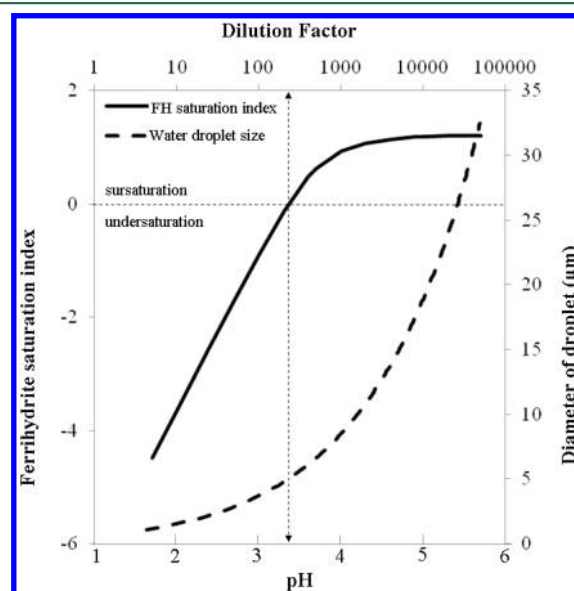


**Figure 4.** Saturation index of Fe in a wet aerosol particle (1 mol L<sup>-1</sup> (NH<sub>4</sub>)<sub>2</sub>SO<sub>4</sub> and 0.05 mol L<sup>-1</sup> H<sub>2</sub>SO<sub>4</sub> solutions after 24 h of reaction; dissolved Fe = 236  $\mu\text{mol L}^{-1}$ ) with respect to fresh ferrihydrite as a function of the dilution factor, assuming a dust particle of 500 nm diameter covered with a 100 nm layer of water and representing a CCN being activated into a cloud droplet of different sizes.

Overall, the Fe<sup>3+</sup> saturation concentration was reached for a 200–400 times dilution (equivalent to pH 3.3–3.6). Below this dilution threshold, Fe<sup>3+</sup> remained in its aqueous form, while at dilutions greater than 400 times (i.e., during the cloud droplet growth stage), precipitation of Fe-NPs will start. A dilution by 200–400 times corresponds to a water layer between 2.2 and 2.8  $\mu\text{m}$  around an initial spherical cloud condensation nuclei (CCN)/dust particle assuming an average diameter of dust particles of 500 nm, with an aqueous coating of 100 nm. This

corresponds to a droplet of 5–6  $\mu\text{m}$  in diameter (see Figure 4). It is noted that natural conditions are likely to be more variable than in the above experiments and simulations (Figure 3). No data exist on mass of dust content in dusty clouds, but an average value of 50 mg dust per liter of water was reported in dusty rains, although this can be highly variable.<sup>34</sup> Furthermore, the water volume fractions in aerosols range from 0.1 to 0.5,<sup>35</sup> and thus, the dilution factors needed for the transition from a typical wet aerosol particle into a cloud droplet is usually in the order of 100,000.

For any given wet aerosol particle activated into a cloud droplet, the amount of Fe-NPs formed will depend primarily on pH, dissolved Fe concentration (itself controlled by the duration of the wet aerosol stage), the dilution ratio, and the potential presence of Fe-binding ligands. Refractory Fe phases in dust are unlikely to dissolve under most cloud conditions because of their high stability/low solubility at near-neutral pH.<sup>25</sup> However, organic compounds, such as oxalates, can increase the fractional Fe solubility of Fe-bearing minerals at acidic pH via aqueous surface-catalyzed dissolution.<sup>36,37</sup> Photoreduction can also affect Fe redox chemistry and fractional Fe solubility<sup>28,37,5</sup> although less dramatically than the effect of acids. Thus, our study probably underestimates the extent of Fe dissolution during the wet aerosol stage. It has been suggested that aerosol processes may increase the dust Fe solubility by tens of times;<sup>38</sup> however, those aerosol samples that have fractional Fe solubility more than 5% are likely to be associated with combustion aerosol.<sup>38</sup>

Interestingly, for the Tibesti sample, comparing the Fe dissolution curve obtained in a continuously reacted experiment<sup>25</sup> at pH = 1 (at a 60 mg L<sup>-1</sup> dust load) with the cumulative curve of dissolved Fe concentration of the cycled experiment between pH 1 and 5–6 (after removing the near-neutral pH time frames shown in Figure 1c) shows a relatively close correspondence (Figure 1d). Similar trends were observed between the continuous dissolution at pH 1 and the pH cycling experiment between pH 1 and pH 5–6 for the Beijing sample. It is clear that although the cycling through the near-neutral pH, cloud droplet stage temporarily stops Fe dissolution, this process in itself has little effect on the final concentration of Fe dissolved during the wet aerosol stages. Therefore, we suggest that during long-range transport clouds halt the Fe dissolution.

One of the important parameters controlling the potentially bioavailable Fe (i.e., combined dissolved Fe and Fe-NPs) from dust is the length of time that the particles persist as wet aerosol. The amount of potentially bioavailable Fe delivered to the ocean is similar whether it is delivered through wet (cloud) or dry (aerosol) deposition though the fraction of soluble Fe versus Fe-NP can be significantly different. The period of time that a given dust particle spent in clouds does not directly affect the total potentially bioavailable Fe. On the other hand, any acid uptake within the clouds will further enhance the acidity of remaining fluid during the wet aerosol phases and, hence, is likely to cause an increase in the dissolved Fe concentration.

## AUTHOR INFORMATION

### Corresponding Author

\*E-mail: z.shi@bham.ac.uk.

### Notes

The authors declare no competing financial interest.

## ACKNOWLEDGMENTS

The manuscript was written through contributions of all authors. All authors have given approval to the final version of the manuscript. Z.S., M.D.K., and S.B. conceived the project, designed the study, carried out most of the data analysis, and wrote the manuscript. L.G.B. advised on methods and interpretation and assisted in the writing of the manuscript. This work was financially supported by the UK Natural Environment Research Council (NE/I021616/1, NE/K000845/1, Shi; NE/E011470/1, Krom) and the University of Birmingham Fellowship scheme (Shi).

## REFERENCES

- (1) Martin, J. H. Glacial-interglacial CO<sub>2</sub> change: the iron hypothesis. *Paleoceanography* **1990**, *5*, 1–13.
- (2) Boyd, P. W.; Ellwood, M. J. The biogeochemical cycle of iron in the ocean. *Nat. Geosci.* **2010**, *3*, 675–682.
- (3) Jickells, T. D.; An, Z. S.; Andersen, K. K.; Baker, A. R.; Bergametti, G.; Brooks, N.; Cao, J. J.; Boyd, P. W.; Duce, R. A.; Hunter, K. A.; Kawahata, H.; Kubilay, N.; LaRoche, J.; Liss, P. S.; Mahowald, N.; Prospero, J. M.; Ridgwell, A. J.; Tegen, I.; Torres, R. Global iron connections between desert dust, ocean biogeochemistry, and climate. *Science* **2005**, *308*, 67–71.
- (4) Mahowald, N. M.; Baker, A. R.; Bergametti, G.; Brooks, N.; Duce, R. A.; Jickells, T. D.; Kubilay, N.; Prospero, J. M.; Tegen, I. Atmospheric global dust cycle and iron inputs to the ocean. *Global Biogeochem. Cycles* **2005**, *19*, GB4025.
- (5) Shi, Z.; Krom, M.; Jickells, T.; Bonneville, S.; Carslaw, K. S.; Mihalopolous, N.; Baker, A. R.; Benning, L. G. Impacts on iron solubility in the mineral dust by processes in the source region and the atmosphere: A review. *Aeolian Res.* **2012**, *5*, 21–42.
- (6) Nodwell, L. M.; Price, N. M. Direct use of inorganic colloidal iron by marine mixotrophic phytoplankton. *Limnol. Oceanogr.* **2001**, *46*, 765–777.
- (7) Sugie, K.; Nishioka, J.; Kuma, K.; Volkov, Y. N.; Nakatsuka, T. Availability of particulate Fe to phytoplankton in the Sea of Okhotsk. *Mar. Chem.* **2013**, *152*, 20–31.
- (8) Shaked, Y.; Lis, H. Disassembling iron availability to phytoplankton. *Front. Microbiol.* **2012**, *3*, Article 123, 1–26.
- (9) Rubin, M.; Berman-Frank, I.; Shaked, Y. Dust- and mineral-iron utilization by the marine dinitrogen-fixer *Trichodesmium*. *Nat. Geosci.* **2011**, *4*, 529–534.
- (10) Shi, Z.; Zhang, D.; Hayashi, M.; Ogata, H.; Ji, H.; Fujie, W. Influences of sulfate and nitrate on the hygroscopic behaviors of coarse dust particles. *Atmos. Environ.* **2008**, *42*, 822–827.
- (11) Manktelow, P. T.; Carslaw, K. S.; Mann, G. W.; Spracklen, D. V. The impact of dust on sulfate aerosol, CN and CCN during an East Asian dust storm. *Atmos. Chem. Phys.* **2010**, *10*, 365–382.
- (12) Kumar, P.; Sokolik, I. N.; Nenes, A. Measurements of cloud condensation nuclei activity and droplet activation kinetics of fresh unprocessed regional dust samples and minerals. *Atmos. Chem. Phys.* **2011**, *11*, 3527–3541.
- (13) Twohy, C. H.; Kreidenweis, S. M.; Eidhammer, T.; Browell, E. V.; Heymsfield, A. J.; Bansemir, A. R.; Anderson, B. E.; Chen, G.; Ismail, S.; DeMott, P. J.; Van Den Heever, C. Saharan dust particles nucleate droplets in eastern Atlantic clouds. *Geophys. Res. Lett.* **2009**, *36*, L01807 DOI: 10.1029/2008GL035846.
- (14) Tian, Y.; Carlton, A. G.; Seitzinger, S. P.; Turpin, B. J. SOA from methylglyoxal in clouds and wet aerosols: measurement and prediction of key products. *Atmos. Environ.* **2010**, *44*, 5218–5226 DOI: 10.1016/j.atmosenv.2010.08.045.
- (15) Facchini, M. C.; Decesari, S.; Mircea, M.; Fuzzi, S.; Loggion, G. Surface tension of atmospheric wet aerosol and cloud/fog droplets in relation to their organic carbon content and chemical composition. *Atmos. Environ.* **2000**, *34*, 4853–4857 DOI: 10.1016/S1352-2310(00)00237-5.

- (16) Seinfeld, J.; Pandis, S. *Atmospheric Physics and Chemistry: From Air Pollution to Climate Change*, 2nd ed.; John Wiley & Sons: New York, 2006.
- (17) Pruppacher, H. R.; Jaenicke, R. The processing of water vapour and aerosols by atmospheric clouds, a global estimate. *Atmos. Res.* **1995**, *38*, 1–4 DOI: 10.1016/0169-8095(94)00098-X.
- (18) Falconer, R. E.; Falconer, P. D. Determination of cloud water acidity at a Mountain Observatory in the Adirondack Mountains of New York state. *J. Geophys. Res. C* **1980**, *85*, 7465–7470.
- (19) Deguillaume, L.; Leriche, M.; Desboeufs, K.; Mailhot, G.; George, C.; Chaumerliac, N. Transition metals in atmospheric liquid phases: sources, reactivity, and sensitive parameters. *Chem. Rev.* **2005**, *105*, 3388–3431.
- (20) Zhu, X.; Prospero, J. M.; Millero, F. J.; Savoie, D. L.; Brass, G. W. The solubility of ferric ion in marine mineral aerosol solutions at ambient relative humidities. *Mar. Chem.* **1992**, *38*, 91–107.
- (21) Meskhidze, N.; Chameides, W. L.; Nenes, A.; Chen, G. Iron mobilization in mineral dust: Can anthropogenic SO<sub>2</sub> emissions affect ocean productivity? *Geophys. Res. Lett.* **2003**, *30*, 2085.
- (22) Ito, A.; Feng, Y. Role of dust alkalinity in acid mobilization of iron. *Atmos. Chem. Phys.* **2010**, *10*, 9237–9250.
- (23) Spokes, J. L.; Jickells, T. D.; Lim, B. Solubilisation of aerosol trace metals by cloud processing: A laboratory study. *Geochim. Cosmochim. Acta* **1994**, *58*, 3281–3287.
- (24) Mackie, D. S.; Boyd, P. W.; Hunter, K. A.; McTainsh, G. H. Simulating the cloud processing of iron in Australian dust: pH and dust concentration. *Geophys. Res. Lett.* **2005**, *32*, L06809.
- (25) Shi, Z.; Bonneville, S.; Krom, M.; Carslaw, K.; Jickells, T.; Baker, A.; Benning, L. Iron dissolution kinetics of mineral dust at low pH during simulated atmospheric processing. *Atmos. Chem. Phys.* **2011**, *11*, 995–1007.
- (26) Desboeufs, K. V.; Losno, R.; Colin, J. L. Factors influencing aerosol solubility during cloud processes. *Atmos. Environ.* **2001**, *35*, 3529–3537.
- (27) Cwiertny, D. M.; Baltrusaitis, J.; Hunter, G. J.; Laskin, A.; Scherer, M. M.; Grassian, V. H. Characterization and acid-mobilization study of iron-containing mineral dust source materials. *J. Geophys. Res.* **2008**, *113*, D05202.
- (28) Fu, H.; Cwiertny, D. M.; Carmichael, G. R.; Scherer, M. M.; Grassian, V. H. Photoreductive dissolution of Fe-containing mineral dust particles in acidic media. *J. Geophys. Res.* **2010**, *115*, D11304.
- (29) Ginoux, P.; Prospero, J. M.; Gill, T. E.; Hsu, C.; Zhao, M. Global scale attribution of anthropogenic and natural dust sources and their emission rates based on MODIS Deep Blue aerosol products. *Rev. Geophys.* **2012**, *50*, RG3005.
- (30) Shi, Z.; Krom, M.; Bonneville, S.; Baker, A.; Jickells, T.; Benning, L. Formation of iron nanoparticles and increase in iron reactivity in the mineral dust during simulated cloud processing. *Environ. Sci. Technol.* **2009**, *43*, 6592–6596.
- (31) Kadar, E.; Cunliffe, M.; Fisher, A.; Stople, B.; Lead, J.; Shi, Z. Chemical interaction of atmospheric mineral dust-derived nanoparticles with natural seawater-EPS and sunlight-mediated changes. *Sci. Total Environ.* **2014**, *468–469*, 265–271.
- (32) Viollier, E.; Inglett, P. W.; Hunter, K.; Roychoudhury, A. N.; Van Cappellen, P. The ferrozine method revisited: Fe(II)/Fe(III) determination in natural waters. *Appl. Geochem.* **2000**, *15*, 785–790.
- (33) Bonneville, S.; Behrends, T.; Van Cappellen, P. Solubility and dissimilatory reduction of iron(III) oxyhydroxides: A linear free energy relationship. *Geochim. Cosmochim. Acta* **2009**, *73*, 5273–5282.
- (34) Theodosi, C.; Markaki, Z.; Mihalopoulos, N. Iron speciation, solubility and temporal variability in wet and dry deposition in the Eastern Mediterranean. *Mar. Chem.* **2010**, *120*, 100–107.
- (35) van Beelen, A. J.; Roelofs, G. J. H.; Hasekamp, O. P.; Henzing, J. S.; Röckmann, T. Estimation of aerosol water and chemical composition from AERONET at Cabauw, the Netherlands. *Atmos. Chem. Phys.* **2014**, *14*, 5960–5987.
- (36) Paris, R.; Desboeufs, K. V. Effect of atmospheric organic complexation on iron-bearing dust solubility. *Atmos. Chem. Phys.* **2013**, *14*, 4895.
- (37) Zhu, X.; Prospero, J. M.; Savoie, D. L.; Millero, F. J.; Zika, R. G.; Saltman, E. S. Photoreduction of iron(III) in marine mineral aerosol solutions. *J. Geophys. Res.* **1993**, *98D*, 9309–9046.
- (38) Sholkovitz, E. R.; Sedwick, P. N.; Church, T. M.; Baker, A. R.; Powell, C. F. Fractional solubility of aerosol iron: Synthesis of a global-scale data set. *Geochim. Cosmochim. Acta* **2012**, *173–189* DOI: 10.1016/j.gca.2012.04.022.